

## **General Disclaimer**

### **One or more of the Following Statements may affect this Document**

- This document has been reproduced from the best copy furnished by the organizational source. It is being released in the interest of making available as much information as possible.
- This document may contain data, which exceeds the sheet parameters. It was furnished in this condition by the organizational source and is the best copy available.
- This document may contain tone-on-tone or color graphs, charts and/or pictures, which have been reproduced in black and white.
- This document is paginated as submitted by the original source.
- Portions of this document are not fully legible due to the historical nature of some of the material. However, it is the best reproduction available from the original submission.

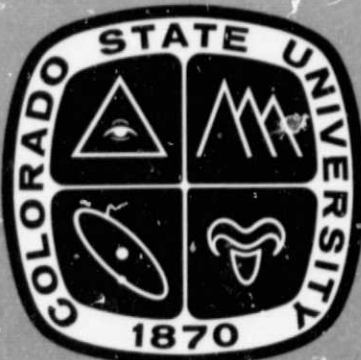
(NASA-CR-158761) NUMERICAL SIMULATION OF  
VTPR TEMPERATURE RETRIEVALS IN A SEVERE  
STORM ENVIRONMENT Final Report, 1 Apr. 1978  
- 31 Mar. 1979 (Colorado State Univ.) 38 p  
HC A03/MP A01

N79-27770  
Unclassified  
CSCL 04B G3/47 27926

# NUMERICAL SIMULATION OF VTPR TEMPERATURE RETRIEVALS IN A SEVERE STORM ENVIRONMENT

By

Thomas H. Vonder Haar,  
Principal Investigator  
And  
Donald W. Hillger,  
Co-Investigator



FINAL REPORT  
NASA GRANT NSG-5259  
PERIOD: 1 April 1978 -  
31 March 1979



DEPARTMENT OF ATMOSPHERIC SCIENCE  
COLORADO STATE UNIVERSITY  
FORT COLLINS, COLORADO

NUMERICAL SIMULATION OF VTPR TEMPERATURE  
RETRIEVALS IN A SEVERE STORM ENVIRONMENT

FINAL REPORT

PERIOD: 1 April 1978 - 31 March 1978

for

NATIONAL AERONAUTICS AND SPACE ADMINISTRATION

Grant NSG-5259

by

Thomas H. Vonder Haar, Principal Investigator  
and

Donald W. Hillger, Co-Investigator  
Department of Atmospheric Science  
Colorado State University  
Fort Collins, CO 80523

June 1979

Technical Monitor: Dr. Albert Arking

## ABSTRACT

This is the study of environmental conditions prior to convective development on the Great Plains of the U.S. on one case study day, 24 August, 1975. The tool used was the High-resolution Infrared Radiation Sounder (HIRS) on Nimbus 6. A dual-retrieval scheme was developed to retrieve both lower tropospheric moisture and temperature parameters from the HIRS radiances. Total precipitable water, surface dew point temperatures, and stability indices were analyzed at a resolution of up to 30 Km on this day. Correlations with interpolated NWS rawinsonde values were high and intrinsic noise levels were low. The true quality of the meso-scale analyses, however, is only seen by examining the small scale features at a scale of approximately 100 Km. Perturbations on the dry line feature for this day were seen in the satellite data, although the dry line position was just as easily picked up by surface observations. Convective development 2½ hours later did seem to correlate well with the local maxima of moisture and instability seen in the satellite analyses. Results of this one case study day, therefore, show the need for more analysis and development of this method of using satellite soundings at the mesoscale.

TABLE OF CONTENTS

	Page
1.0 INTRODUCTION. . . . .	1
2.0 FOCUS OF RESEARCH . . . . .	2
3.0 HIRS DUAL RETRIEVAL SCHEME. . . . .	3
4.0 MESOSCALE APPLICATIONS. . . . .	9
5.0 CASE STUDY DAY - 24 AUGUST 1975 . . . . .	12
6.0 ANALYSIS OF VARIABLES . . . . .	16
7.0 MESOSCALE ANALYSIS - 24 AUGUST 1975 . . . . .	19
8.0 CONCLUSIONS . . . . .	26
REFERENCES. . . . .	33

## 1.0 INTRODUCTION

The determination of the quantitative structure of the temperature and moisture environment necessary for severe storm development is a desirable goal. Temperature gradients are important precursors for mechanisms related to severe storm formation. Mixing of atmospheric masses of differing stability may lead to release of potential energy. In a similar manner moisture sources are necessary for the release of latent heat through condensation. Both moist areas of latent energy and the overlying or adjacent dry regions are therefore known to be environmental severe storm indicators. In many cases these indicators are only qualitatively known, since quantitative information about mesoscale (25 + 250 km) weather is scarce except for limited experimental monitoring associated with such programs as the Severe Environmental Storms and Mesoscale Experiment (Project SESAME 1976, Lilly 1975 and 1977).

The first goal of the SESAME project relates directly to determination of such environmental parameters mentioned above and their relation to intensity of severe storm development. A second goal is to test the ability of new remote sensing systems as applied to such mesoscale problems. The satellite data used in this study is such a remote sensing system which has been around for several years. Supposed failures of using satellite soundings in many cases (Tracton and McPherson 1977) may be due to its improper use (Kelly, et al 1978). The development and use of high-resolution temperature and moisture fields as derived from satellite soundings for mesoscale applications may be a proper use of such information. The satellite sounder inherently provides better horizontal resolution and coverage than its counterpart the rawinsonde. Therefore it is reasonable to use the satellite data in such a high-resolution mode

to test its true ability as an instrument to provide mesoscale weather parameters.

## 2.0 FOCUS OF RESEARCH

The original intent of this research proposal was to focus on known severe storm environments. Satellite data such as obtained from the Vertical Temperature Profile Radiometer (VTPR), an early 1970's instrument, would be simulated to determine how this data could be better interpreted in such situations. However, the early results of such simulation proved as confusing as the data in actual severe storm cases. The confusion lies in the inability to determine both temperature and moisture parameters from a basically temperature-only sensing instrument (only one  $H_2O$  and one window channel in the VTPR). The further improvement of satellite instruments in the late 1970's has introduced the Nimbus-6 High-resolution Infrared Radiation Sounder, HIRS (Smith, et al., 1975), with at least 2 water vapor channels and 2 infrared window channels. The radiances in these spectral regions are predominant in the moisture determination process. Since the use of this new instrument made the older generation data obsolete, it was decided to explore this new data set.

The HIRS instrument has the capability of determining both temperature and moisture parameters from separate but not independent spectral regions. Therefore, the use of this data was explored. Part of the process required the development of a dual retrieval scheme designed for this type of instrument but not exclusively for this instrument. Such a scheme or algorithm can be applied to TIROS-N/HIRS-2 sounding data (Schwab 1978) which as of fall 1978 is the operational polar-orbiting sounder replacing the older NOAA/VTPR series of sounders.

It must also be remembered that working with real data at the mesoscale has its merits in that only a few studies have been done in that area (Smith et al., 1978)(Wark, et al., 1974). Much simulation has been done to select the channels for such an instrument as HIRS. It is now necessary to determine the basic limitations of such an instrument. Limitations in terms of noise levels of derived parameters and the resolution necessary for adequate temperature and moisture discrimination have been accomplished for the VTPR instrument (Hillger and Vonder Haar, 1979). These results show that the satellite sounder is capable of detecting the same temperature gradient information as mesoscale rawinsonde soundings. However, the VTPR instrument was inadequate for mesoscale moisture determination compared to mesoscale rawinsondes. The higher vertical resolution of the rawinsonde soundings was their main advantage. The determination of mesoscale moisture from VTPR data is only possible if the temperature structure is known beforehand.

The same study of basic limitations in real case-study data has been accomplished here for fields of temperature and moisture information derived from the HIRS satellite sounder. The number of case study days is not large but the results are encouraging.

### 3.0 HIRS DUAL RETRIEVAL SCHEME

The problem of not being able to determine both the temperature and moisture structure from a set of  $\text{CO}_2$  radiances from the VTPR instrument was its most basic limitation. In trying to derive the temperature structure or gradient across a field of data the undetermined effect of hidden moisture gradients was a problem. There was no way of easily determining whether one region was actually warmer or drier than an adjacent region, since the two effects were similarly sensed by the

observed radiances. This same problem appears in surface temperature determination, which is part of the task here. In order to determine the surface temperature the amount of the absorbing gas (mostly water vapor in the case of window channels) must be known, or to determine the absorbing gas content the underlying surface temperature must be known. The problem does have a solution if enough pieces of partially-independent information are available. Groundwork for such methods is not new. (Smith, 1970). However, as applied to this problem we must get down to specifics.

Basically three things were desired to be known from the satellite-sensed radiances. The temperature profile, moisture profile, and the surface temperature are all major influences upon the radiances. The determination of these three things required radiances from both a molecular absorption band of constant mixing ratio such as  $\text{CO}_2$  and an  $\text{H}_2\text{O}$  band where the amount of absorber is desired, as well as a window channel which is fairly free of any molecular absorption. These three requirements were met by the HIRS instrument with a set of  $15 \mu\text{m}$   $\text{CO}_2$  channels (or alternately  $4.3 \mu\text{m}$   $\text{CO}_2$  channels); a  $6.7 \mu\text{m}$  and an  $8.2 \mu\text{m}$   $\text{H}_2\text{O}$  channel as well as two window channels at  $3.7 \mu\text{m}$  and  $11 \mu\text{m}$ . While the  $\text{CO}_2$  channels were used for temperature determination, the  $\text{H}_2\text{O}$  channels provided moisture determination in at least two levels roughly separated by the 600 mb level. The window channel, however, was of primary importance in determining the background surface term in the radiative transfer calculation. This is especially true in determining temperature and moisture parameters from spectral regions with large transmittances at the surface (low absorbtion).

The HIRS channels are shown in Figure 1 and are listed in Table 1. In using the information from these channels a priority system had to be

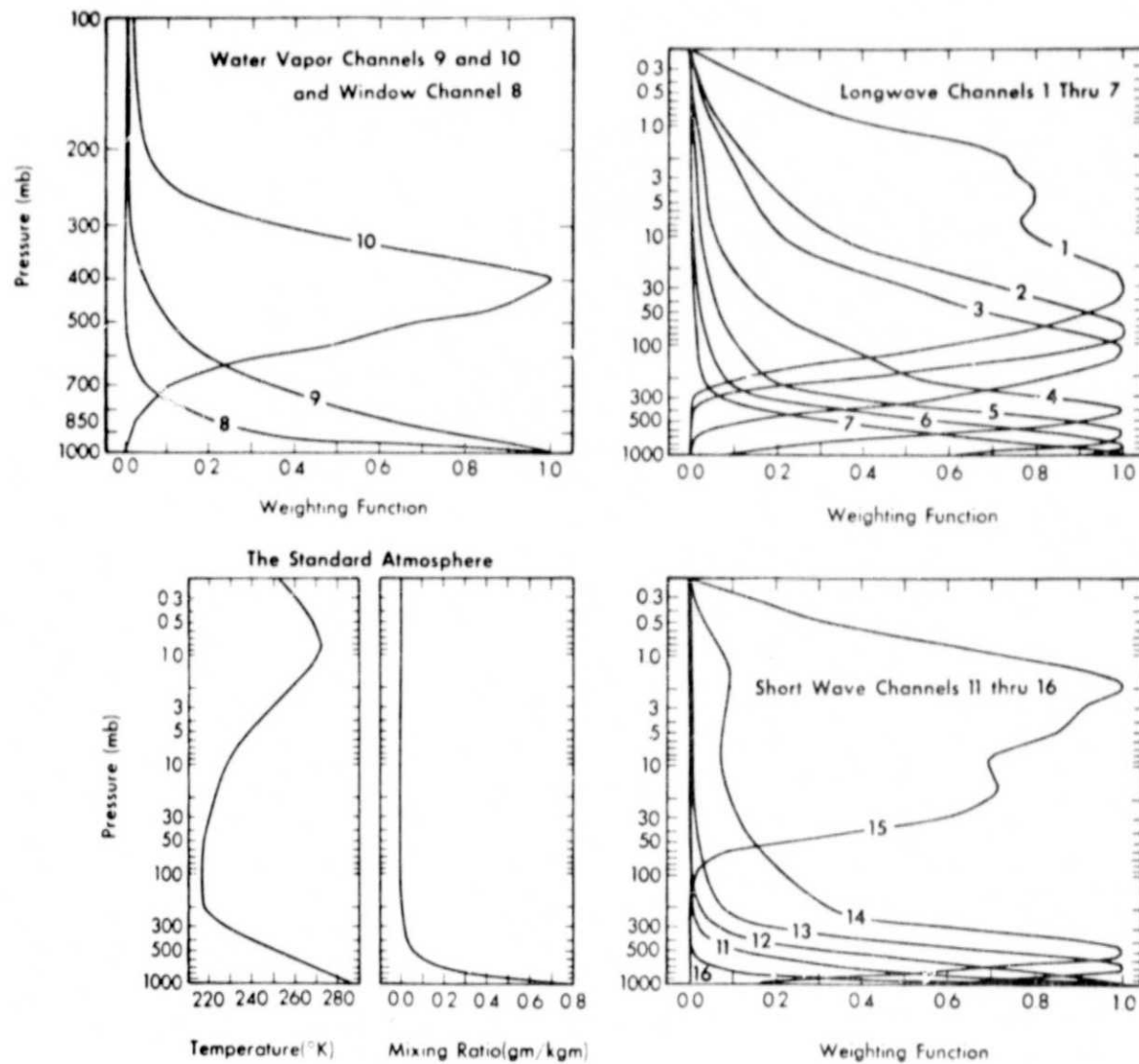


Figure 1. Weighting functions for the HIRS temperature and water vapor channels. (The Nimbus-6 User's Guide).

Table 1.  
(The Nimbus-6 User's Guide)

Functions of the HIRS Channels

Channel Number	Channel Central Wave-number	Central Wavelength ( $\mu\text{m}$ )	Principal Absorbing Constituents	Level of Peak Energy Contribution	Purpose of the Radiance Observation
1	668	15.0	$\text{CO}_2$	30 mb	Temperature Sounding. The 15 $\mu\text{m}$ band channels provide better sensitivity to the temperature of relatively cold regions of the atmosphere than can be achieved with the 4.3 $\mu\text{m}$ band channels.
2	679	14.7	$\text{CO}_2$	60 mb	
3	690	14.4	$\text{CO}_2$	100 mb	
4	702	14.2	$\text{CO}_2$	250 mb	
5	716	14.0	$\text{CO}_2$	500 mb	
6	733	13.6	$\text{CO}_2/\text{H}_2\text{O}$	750 mb	
7	749	13.4	$\text{CO}_2/\text{H}_2\text{O}$	900 mb	Radiances in Channels 5, 6, and 7 are also used to calculate the heights and amounts of cloud within the HIRS field of view.
8	900	11.0	Window	Surface	Surface Temperature and cloud detection.
9	1224	8.2	$\text{H}_2\text{O}$	900 mb	Water Vapor Sounding. Provide water vapor corrections for $\text{CO}_2$ and window channels.
10	1496	6.7	$\text{H}_2\text{O}$	400 mb	The 6.7 $\mu\text{m}$ channel is also used to detect thin cirrus cloud.
11	2190	4.57	$\text{N}_2\text{O}$	950 mb	Temperature Sounding. The 4.3 $\mu\text{m}$ band channels provide better sensitivity to the temperature of relatively warm regions of the atmosphere than can be achieved with the 15 $\mu\text{m}$ band channels.
12	2212	4.52	$\text{N}_2\text{O}$	850 mb	
13	2242	4.46	$\text{CO}_2/\text{N}_2\text{O}$	700 mb	
14	2275	4.40	$\text{CO}_2/\text{N}_2\text{O}$	600 mb	
15	2357	4.24	$\text{CO}_2$	5 mb	Also, the short-wavelength radiances are less sensitive to clouds than those for the 15 $\mu\text{m}$ region.
16	2692	3.71	Window	Surface	Surface Temperature. Much less sensitive to clouds and $\text{H}_2\text{O}$ than 11 $\mu\text{m}$ window. Used with 11 $\mu\text{m}$ channel to detect cloud contamination and derive surface temperature under partly cloudy sky conditions.
17	14,443	0.69	Window	Cloud	Cloud Detection. Used during the day with 3.7 $\mu\text{m}$ and 11 $\mu\text{m}$ window channels to define clear fields of view and to specify any reflected solar contributions to the 3.7 $\mu\text{m}$ channel.

followed. The determination of the surface boundary term was considered the most important and could be easily accomplished using the highly transparent 3.7  $\mu\text{m}$  window channel. To do this a temperature profile was assumed (initial guess) and the surface term was determined as a residual to match the observed window channel radiance. The next step was to adjust the initial guess moisture content and therefore the transmittance according to the observed radiances in the two  $\text{H}_2\text{O}$  channels. The third step then involved adjusting the initial guess temperature profile according to the  $\text{CO}_2$  channels. The last two steps were then repeated as long as convergence was assured. Usually as few as 2 to 3 complete cycles or iterations were required to obtain a temperature and moisture profile which provided radiances through radiative transfer calculations similar to those observed. The residuals between observed and calculated radiances were required to decrease as a convergence criteria. This scheme is basically iterative and is much faster than previous schemes used with VTPR data (Hillger and Vonder Haar, 1977) which determined primarily temperature profiles and total precipitable water secondarily as a residual in the process.

The determination of the surface temperature as a residual in the radiative transfer calculations follows a formula which was applied only once as the first step in the retrieval of atmosphere parameters for each scan spot of the satellite.

$$B(T'_{\text{sfc}}, \nu) = B(T_{\text{sfc}}, \nu) + (R_{\text{obs}} - R_{\text{calc}})/\tau_s(\nu, T_o(x), Q_o(x)) \quad (1)$$

By inverting this equation we can see that the desired surface temperature  $T'_{\text{sfc}}$  is the correct factor to make the calculated radiance,  $R_{\text{calc}}$ , in the window channel at wavenumber  $\nu$  equal the observed radiance,  $R_{\text{obs}}$ . This assumes that the atmospheric temperature and moisture structure are

either correct or that unknown small differences are of minor significance. The idea, therefore, was to have good initial guess temperature,  $T_o(x)$ , and mixing ratio,  $Q_o(x)$  profiles, where  $x$  is some vertical coordinate, in order to initially determine the approximate atmospheric transmittance at the surface,  $\tau_s$ . In the case here a composite rawinsonde from a time period near the satellite pass was used.

Moisture feedback was accomplished through the relaxation formula for iteration  $n + 1$

$$Q^{(n+1)}(x) = Q^{(n)}(x) \left[ 1 - \alpha \sum_{i=1}^2 \left( \frac{R_{\text{obs},i} - 1}{R_{\text{calc},i}^{(n)}} \right) W_i^{(n)}(x) \right] \quad (2)$$

and applies to the mixing ratio  $Q(x)$  at any level  $x$ . There are two  $H_2O$  channels represented by the subscript  $i$ , and the weight  $W_i$  applied to each radiance channel is just the derivative of the transmittance of that level  $\tau(x)$ . Each  $H_2O$  channel will perturb the mixing ratio profile  $Q(x)$  at the levels  $x$  where its weighting function  $W(x)$  is the non-zero. The factor  $\alpha$  is necessary because of the change in units from radiance to mixing ratio. It approximates  $\frac{\Delta Q}{Q} \cdot \frac{R}{\Delta R}$  or  $\frac{\% \Delta Q}{\% \Delta R}$ . In this case a factor of 5 was chosen to approximate this change in units and to speed convergence. The negative sign in equation 2 says that an increase in radiance is associated with a decrease in moisture.

In a similar manner the temperature feedback followed a modified relaxation formula of Smith's (1970).

$$B(T^{(n+1),v}) = B(T^{(n),v}) \left[ 1 + \sum_{i=1}^4 \left( \frac{R_{\text{obs},i} - 1}{R_{\text{calc},i}^{(n)}} \right) W_i^{(n)}(x) \right] \quad (3)$$

For one channel this formula reduces directly to that of Smith, but his method averaged the resulting independent temperature determinations

from each channel in a similar manner to the way the blackbody radiances are averaged here. This short cut greatly reduced the number of calculations. The four most transparent 15  $\mu\text{m}$   $\text{CO}_2$  absorption channels were used to try to retrieve the tropospheric temperature profile for each scan spot.

These last two iterative relaxation formulas were applied alternately as long as convergence is maintained. A decrease in the root mean square radiance residual between observed and calculated radiance is the necessary criteria.

$$\Delta R_{\text{rms}}^{(n)} = \sqrt{\frac{1}{N} \sum_{i=1}^N \left[ R_{\text{obs},i} - R_{\text{calc},i}^{(n)} \right]^2} \quad (4)$$

The number of channels N included the 2 window, 2  $\text{H}_2\text{O}$ , and 4  $\text{CO}_2$  channels which were used in the retrieval process. Only the 4 most transparent  $\text{CO}_2$  channels were used in the retrieval scheme because mainly lower tropospheric temperature and moisture variables were desired. These 4 channels each have weighting function maxima below the tropopause as do the 2  $\text{H}_2\text{O}$  channels.

#### 4.0 MESOSCALE APPLICATIONS

In developing and applying this dual retrieval scheme there were two objectives in mind. One was to determine parameters which could aid in severe storm forecasting. The second was to determine these parameters at a scale which would be useful for mesoscale applications. The first objective was met by emphasising the retrieval of surface and lower tropospheric parameters from the HIRS radiances. The second was accomplished by determining these parameters at the full resolution of the VTPR instrument of about 30 Km.

The analysis and forecasting parameters which proved to be the easiest to determine from the satellite sounding radiances were the total precipitable water and the atmospheric stability of the sounded column. The total precipitable water gives a measure of the amount of latent energy in severe storm situations. Few storms develop to the severe stage without a sufficient energy source in terms of adequate low-level moisture. Likewise, atmospheric stability indices such as the totals indices have been used for many years (Miller 1972) as good indicators of severe weather potential. These indices are measures of surface heating and moisture as well as atmospheric instability or the potential for release of such sources of sensible and latent energy. The total precipitable water was determined from satellite radiances in the two  $H_2O$  channels which can sense moisture in two layers roughly separated by the 600 mb level. These two channels were then used as a pair to determine the total atmospheric water. The procedure is through the changing of the initial guess mixing ratio profile where the two  $H_2O$  weighting functions are non-zero. The amount of change for each channel depends on the amplitude of the weighted function, with maximum change occurring at the weighting function maxima for each channel. However, since the weighting functions are broad the range occurs over a large vertical depth, and this approximates a change in the total precipitable water in two layers.

The determination of stability indices was a by-product of the dual retrieval process. The atmospheric stability indices to be determined depend only on temperature and moisture parameters at various standard levels. Both the totals index and the K value rely on temperature and dew point temperature at the 850 mb level and the 500 mb temperature.

The K value also incorporates the 700 mb temperature and dew point temperature. Their formulas follow.

$$\text{Vertical Total} = T_{850} - T_{500} \quad (5)$$

$$\text{Cross Total} = Td_{850} - T_{500} \quad (6)$$

$$\text{Total Totals} = \text{Vertical Total} + \text{Cross Total} \quad (7)$$

$$\text{K Value} = T_{850} + Td_{850}$$

$$-(T_{700} - Td_{700}) - T_{500} \quad (8)$$

The five desired parameters are the temperatures at 850, 700, and 500 mb ( $T_{850}$ ,  $T_{700}$ , and  $T_{500}$ ) and the dew point temperatures at 850 and 700 mb ( $Td_{850}$  and  $Td_{700}$ ). The derived temperatures at the standard levels are a result of perturbations on the initial guess temperature profile. The temperature determination at any level is basically a combination of the contribution from each of the temperature-sensing  $\text{CO}_2$  channels. The dew point temperatures, on the other hand, were directly computed from the retrieved mixing ratio profile for each sounding column.

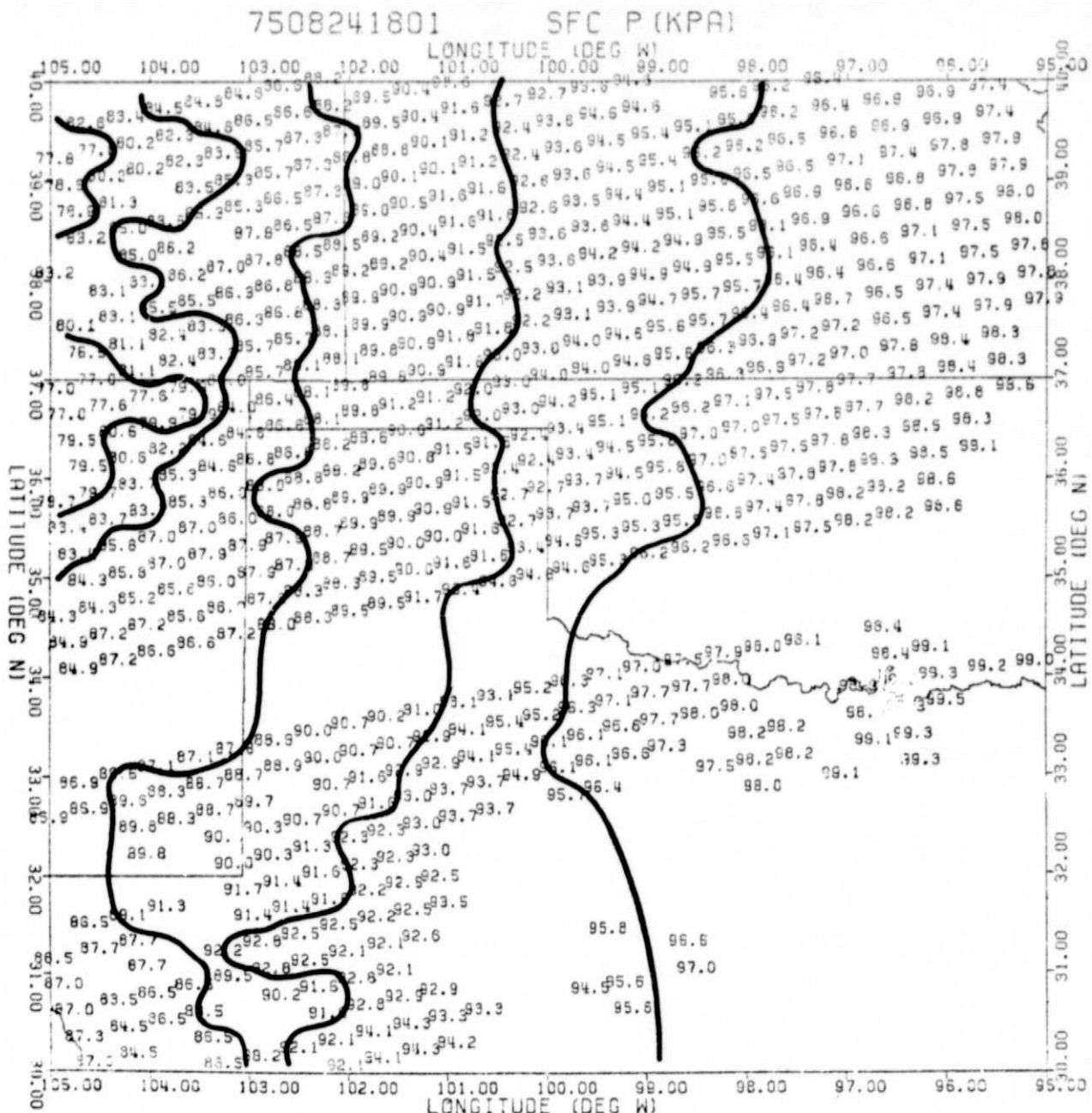
Besides determining these analysis and forecasting parameters, their distribution in space must be known. Storms usually develop along lines which are perpendicular to gradients in temperature or moisture, such as the dry line. From conventional data sources these lines for potential development may appear to be rather uniform, but smaller scale variations along the lines are observed at higher resolution. An objective of this study was to examine the potential for determining these small scale variations from satellite soundings. The satellite data will, therefore, be applied at the mesoscale where its advantage of high-horizontal resolution may be realized.

### 5.0 CASE STUDY DAY - 24 AUGUST 1975

The first HIRS radiances available for study were obtained during the data systems test (DST) period in August and September of 1975 (Gary, 1977). This was shortly after the launch of Nimbus-6. Of these days, one was chosen here for intensive meso-analysis. At least 2 other days in this period had similar near nadir views from Nimbus 6 and could also be studied at a later date.

The region for study is centered on the SESAME mesoscale sounding network in western Oklahoma. The size of the region for study was chosen to be  $10^{\circ}$  latitude by  $10^{\circ}$  longitude ( $30^{\circ}$ - $40^{\circ}$ N and  $95^{\circ}$ - $105^{\circ}$ W). This represents an area of approximately 1000 km on a side. This size allows a study of mesoscale weather over a large region covering most of Kansas, Oklahoma, and northern Texas as shown in Figure 2. The state outlines are shown along with the surface pressure at various points. These surface pressures were calculated by hydrostatic reduction of sea level pressure depending on the terrain elevation above sea level. Each  $.5^{\circ}$  latitude-longitude box had a mean terrain elevation and therefore an equivalent surface pressure assigned to it.

The Nimbus-6 satellite is a polar orbiting satellite with an approximate local noon equator crossing time. At the latitude of study the time on this case study day was 1801 GMT (1201 CST). This time provided a good indication at mid-day weather for subsequent convective activity later in the day. The orbit is ascending and the sub-satellite track falls over the Texas panhandle. Radiances were then sensed in 21 spots on each side of the sub-satellite track at a resolution of approximately 30 km at nadir. Figure 2 shows the spots which fall within the specified boundary. The gap through northern Texas and Oklahoma is a calibration period of the satellite which occurs every 20 scan lines.



**ORIGINAL PAGE IS  
OF POOR QUALITY**

Figure 2. Surface Pressures (kPa) for each retrieved HIRS scan spot at 1801 GMT on 24 August 1975. These values are hydrostatic pressure reductions from sea level for mean surface elevation in .50° lat-lon boxes. Missing soundings are due to a calibration period and cloudiness in Texas. Contours are every 40 kPa.

The other missing data in Figure 2 is due to a cloudy situation in eastern Texas. This is also shown in Figure 3, which is a Synchronous Meteorological Satellite (SMS) visible image at 1745 GMT on this day. No effort was made in this study to sound in cloudy columns. The addition of a cloud model on the incorporation of microwave sounding could be a useful addition. Therefore, only clear columns were chosen for temperature and moisture retrieval.

Two methods were used for cloud detection. The visible channel of HIRS at  $.69\mu\text{m}$  was used to sense reflected solar radiation from the surface of the earth or clouds. If the visible channel radiance exceeded a  $4.5 \text{ mW}/(\text{m}^2 \text{ sr cm}^{-1})$  threshold, clouds were assumed. On this day a maximum of about  $20 \text{ mW}/(\text{m}^2 \text{ sr cm}^{-1})$  was detected, and theoretical calculations indicate that a value of about  $25 \text{ mW}/(\text{m}^2 \text{ sr cm}^{-1})$  would be equivalent to a surface reflectivity or albedo of unity. So the 4.5 value represents an albedo of approximately 20%. This value was also empirically found to be a good threshold by comparison with clouds seen in the SMS visible image.

A second method for detection of cloud or broken surface characteristics was also used. This method relied on the fact that the two HIRS window channels at  $3.7$  and  $11 \mu\text{m}$  respond as different powers of temperature. A uniform field of view in the sounded column would produce an equivalent radiative temperature in each channel, but a non-uniform field of view would produce different equivalent radiative temperatures (Smith et al., 1974). The difference in brightness temperatures was allowed to be as great as  $15^{\circ}\text{C}$  before clouds were considered to be within the field of view. This value allows for the differing atmospheric absorption and emission characteristics in each spectral interval. The use of this

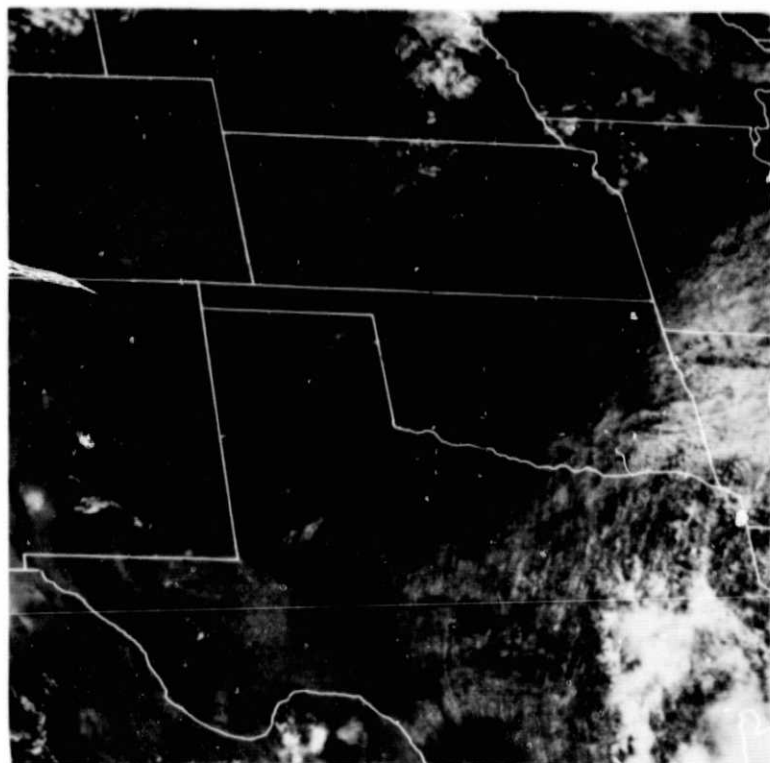


Figure 3 SMS visible image at 1745 GMT (1145 CST) on 24 August 1975. Note almost perfectly clear skies at the time of the Nimbus 6 HIRS soundings.

ORIGINAL PAGE IS  
OF POOR QUALITY

method determined approximately the same cloudy fields of view as the first method but didn't detect small clouds or clouds with fairly uniform cloud tops.

The HIRS visible channel was also used to determine the effect of reflected energy in the 3.7  $\mu\text{m}$  infrared window channel. Calculations show that the amount of solar energy reflected from the surface at 3.7  $\mu\text{m}$  is approximately equal to that lost by the fact that the emissivity of the surface is not unity. Therefore, the problem is not considered significant. A possible effect of an erroneous assumption would be that surface temperature would be too high.

#### 6.0 ANALYSIS OF VARIABLES

The derived variables from the Nimbus-6 radiances are listed in Table 2. These parameters were compared to the same variables interpolated at 1800 GMT from the bordering synoptic NWS rawinsonde sounding times of 1200 GMT before and 0000 GMT after the satellite pass. The correlations are also listed in Table 2. The number of points for comparison is a maximum of 7, one for each rawinsonde site within the region of study, therefore, these numbers should not carry too much weight. In spite of this, the correlations are fairly high especially for the moisture and stability variables. The only gross failure was the 500 mb temperatures which showed little structure in the field above the noise level for this variable.

The noise levels in Table 2 were obtained from a structure function analysis (Gandin 1963) of all the measurements in the area of study. The analysis method was the same as that used by the authors in a previous study of VTPR satellite soundings (Hillger and Vonder Haar, 1979). There were approximately 600 retrieved satellite measurements for each

Table 2  
Variable Correlation and Noise

Variable	Correlation: 1800 GMT interpolated vs 1800 GMT HIRS	RMS Noise	Std. Deviation of Field (Signal)	Signal/ Noise
Total PW	.90	2.21 mm	11.66 mm	5.3
PW above 600 mb	.47	.34 mm	1.52 mm	4.5
Temperatures				
- surface	.75	.93°C	3.67°C	4.0
- 850 mb	.63	.71°C	1.52°C	2.1
- 700 mb	.68	.46°C	.78°C	1.7
- 500 mb	-.62	.38°C	.61°C	1.6
Mixing Ratios				
- sfc	.99	.93 g/kg	4.55 g/kg	4.9
- 850 mb	.75	.68 g/kg	2.53 g/kg	3.7
- 700 mb	.70	.41 g/kg	1.47 g/kg	3.6
Sfc Dew Point Temp	.99	1.27°C	6.88°C	5.4
Vertical Total	.60	.24°C	.35°C	1.5
Cross Total	.80	1.12°C	4.33°C	3.9
Total Totals	.88	1.20°C	4.48°C	3.7
K value	.88	2.24°C	8.46°C	3.8

variable even with cloudy fields of view eliminated from the area of study. So the statistical base for the structure analysis was large. The theory behind determining the noise level for closely spaced data is to extrapolate the difference between the individual measurements as the separation between the measurements is decreased. With 600 points at approximately 30 Km resolution the number of possible pairs of measurements at the minimum separation distance of 30 Km is about 1200 pair. The values listed in Table 2 are the rms differences at this minimum separation distance without extrapolation to zero separation distance. The reason for not extrapolating is that there is no assurance that the difference between the measurements will decrease beyond its value of this minimum separation distance. In other words, the intrinsic noise level may have been obtained regardless of how closely spaced the measurements are.

The values in Table 2 show that temperatures were obtained with a noise level of less than  $1^{\circ}\text{C}$ . This rms noise level, however, does not indicate any bias which might be present in the measurements. These rms noise levels therefore indicate the maximum capabilities of this retrieval scheme as used on HIRS radiance information. These noise levels, however, should be compared to the standard deviation of all the variables in the field in Table 2. These values show the amount of variability in the derived field. The amount of variability depends on both the true variability and the ability to detect that variability, such as gradients in the field. Only if the variability is larger than the noise level for that field will there be significant information in that field, unless, of course, if the true field is flat. There appears to be significant signal above noise for all variables except possibly

the 700 and 500 mb temperature fields and the vertical total index. For these variables the signal to noise ratio is less than 2. All these point to a lack of temperature retrieval ability when compared to the signal above noise for the moisture variables. This is possibly due to the iterative retrieval scheme design which adjusts the initial guess moisture before the temperatures are adjusted. This could possibly make the moisture results improve at the expense of the temperature retrievals. Another explanation is that there is basically much more moisture signal in mesoscale situations than there is a temperature signal, so this retrieval method may be justified. Small scale moisture variations is what is desired in mesoscale prediction where they may be the main predictor.

#### 7.0 MESOSCALE ANALYSIS - 24 AUGUST 1975

Fields of several analysis and forecasting variables will be shown for 1801 GMT on 24 August 1975. The precipitable water analysis in Figure 4 shows a general northwest to southeast moisture gradient, but a secondary maximum does exist in the western part of the Texas panhandle. Nearby gaps in measurements do tell of the existence of some cloudiness at the time of the satellite soundings. However, local maxima of precipitable water do extend up into central Kansas. For comparison the 1801 GMT interpolated rawinsonde precipitable water field is shown in Figure 5. No secondary maxima is shown in this coarser resolution data. It is possible that the resolution difference causes the rawinsonde data to not contain the amount of detail that is in the satellite data. One indication in the rawinsonde soundings in Figure 5 is the large 12 hour precipitable water increase at Midland TX (MAF) which hints that the local maximum in the Texas panhandle at 1801 GMT does still exist at 0000 GMT.

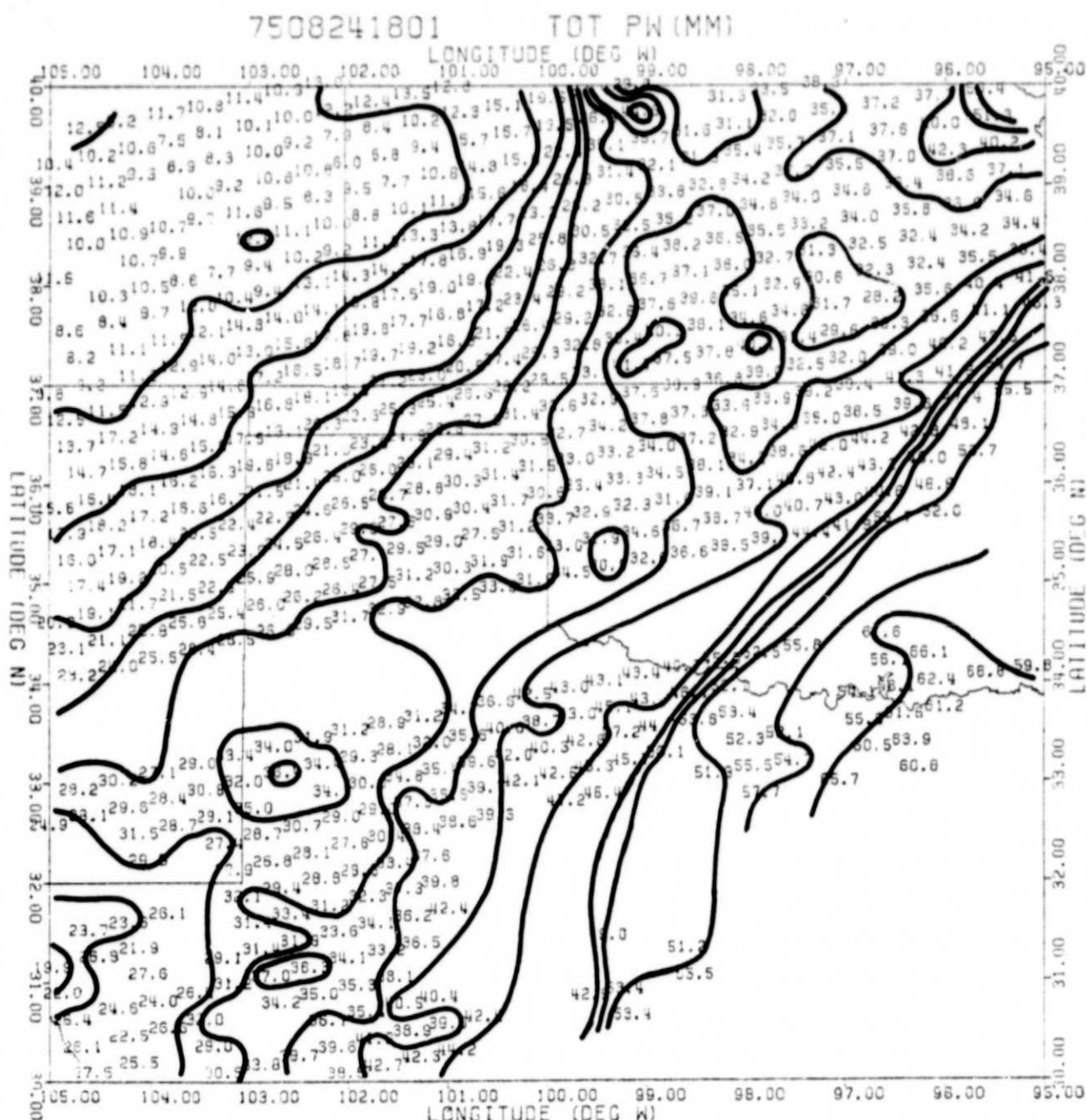
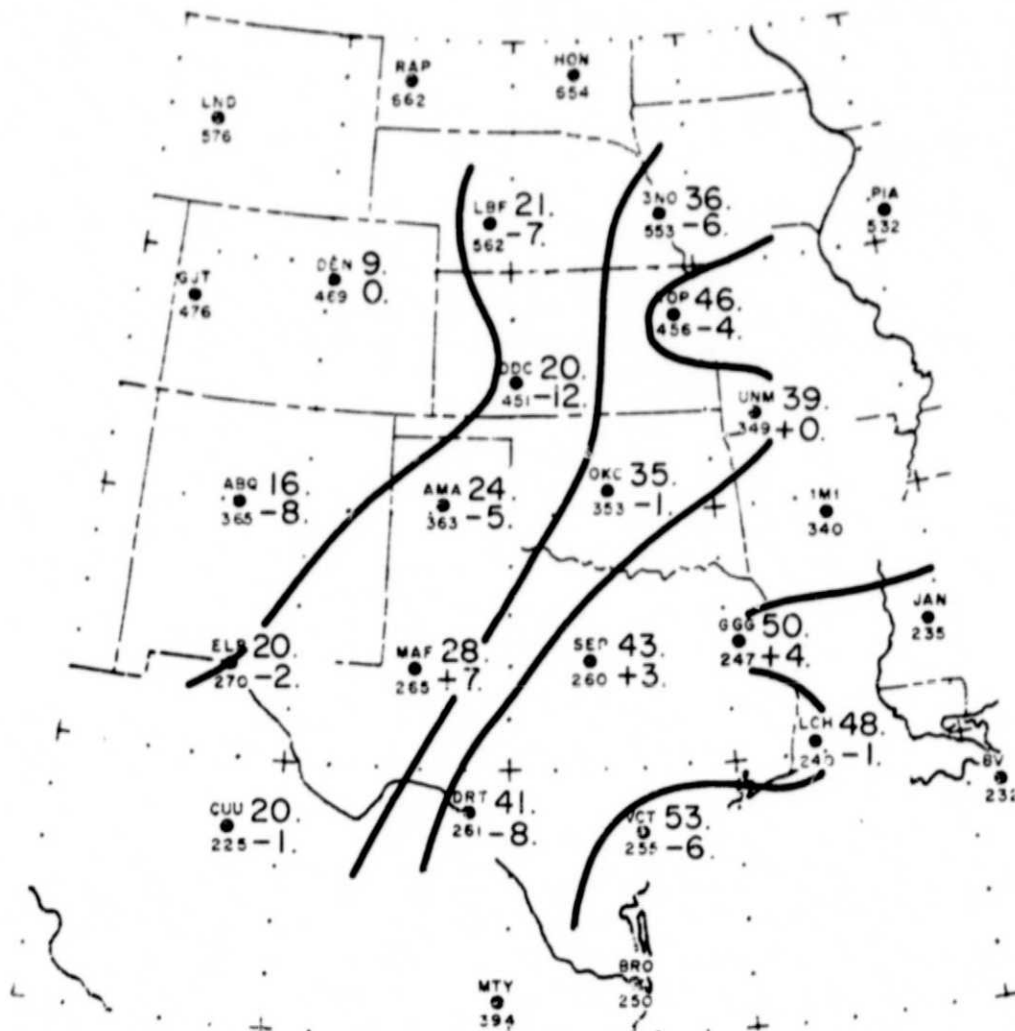


Figure 4. Total precipitable water analysis (mm) from retrieved HIRS soundings at 1801 GMT on 24 August 1975. Note the moisture maximum along the western edge of the Texas panhandle. Contours are every 4 mm.



24 AUG 75  
1800 GMT INTERPOLATED  
PRECIPITABLE WATER (mm)

Figure 5. Total precipitable water analysis from 1800 GMT interpolated values on 24 August 1975 from synoptic rawinsondes at 1200 and 0000 GMT. Upper value is precipitable water, lower value is 12 hour change.

ORIGINAL PAGE IS  
OF POOR QUALITY

An analysis of the satellite-derived surface dew point temperatures in Figure 6 shows the same local maximum in the western Texas panhandle with other maxima extending along a line up through central Kansas. The tightest surface moisture gradient seems to be in northwestern Kansas just to the west of a local surface moisture maximum. The same field of 1800 GMT dew point temperatures are analyzed from surface observing stations is shown in Figure 7. This figure shows a very similar analysis with a general gradient from northwest to southeast. Again the strongest gradient appears to be in the region of northwestern Kansas. This strong gradient is probably the best indication of the dry line feature which frequently exists in the high plains during many days in the summer (Rhea, 1966). Schaefer (1973 and 1974) defined the dry line as the 9g/Kg mixing ratio line which is consistently near the center of the zone of sharpest mixing ratio gradient. The equivalent dew point temperature for saturation at 9g/Kg is about  $12^{\circ}\text{C}$ . This line appears to be in the same position in the analysis for both the satellite and surface data. Also, a bulge or bow in the surface dew point lines in southwest New Mexico as seen from surface observations does give some indication of the secondary maximum in the satellite-derived dew point temperatures.

The satellite analysis seems to show the same general dry line position as the surface observations but with possible local perturbations of maxima such as in the Texas panhandle. To the east of this dry line there later does develop some moderate convection as shown on the 2030 GMT SMS visible image in Figure 8. This occurred about  $2\frac{1}{2}$  hours after the satellite soundings. The convection appears to be the heaviest in the Texas panhandle near or just north of the satellite-derived dew point secondary maximum. Little or no convection occurs behind the dry

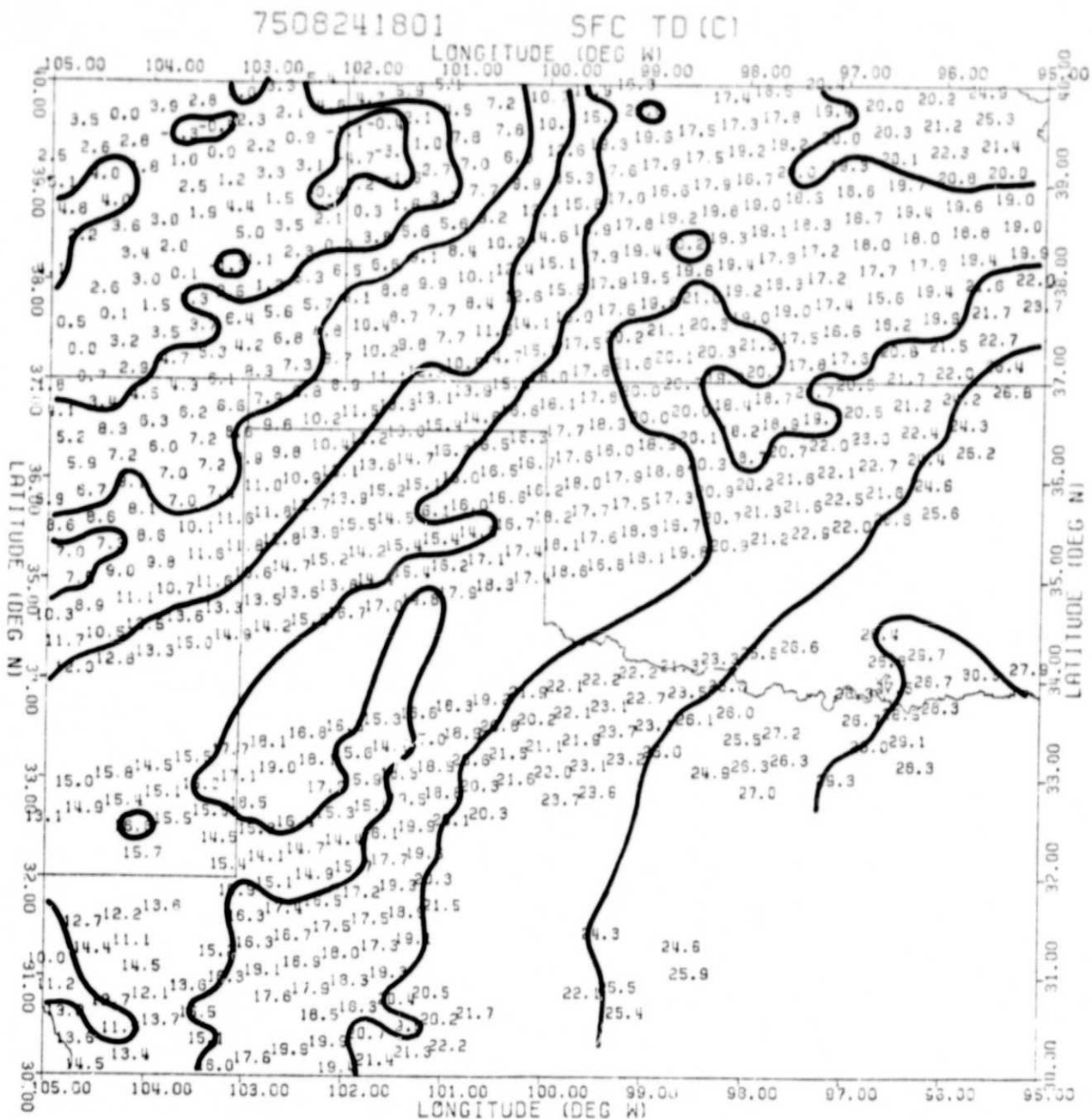


Figure 6. Surface dew point temperature analysis ( $^{\circ}\text{C}$ ) from retrieved HIRS soundings at 1801 GMT on 24 August 1975. Note the moisture maximum in the same position as in the PW analysis in Figure 4. Contours are every  $4^{\circ}\text{C}$ .

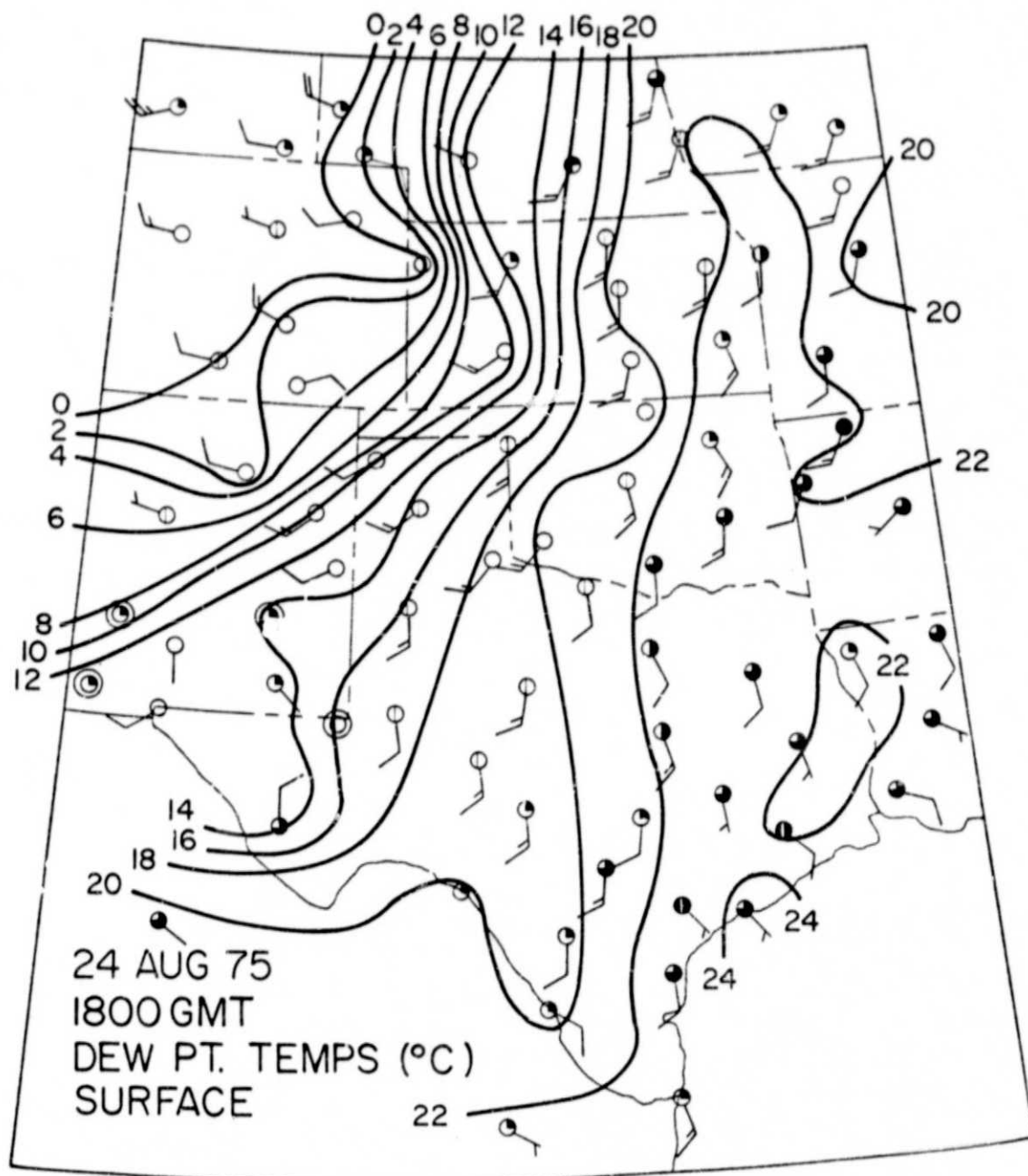


Figure 7. Dew point temperature analysis from surface observations at 1800 GMT (1200 CST) on 24 August 1975. The 9g/kg mixing ratio isohume, usually associated with dry line position, is approximately equivalent to the 12°C dew point isodrosotherm.

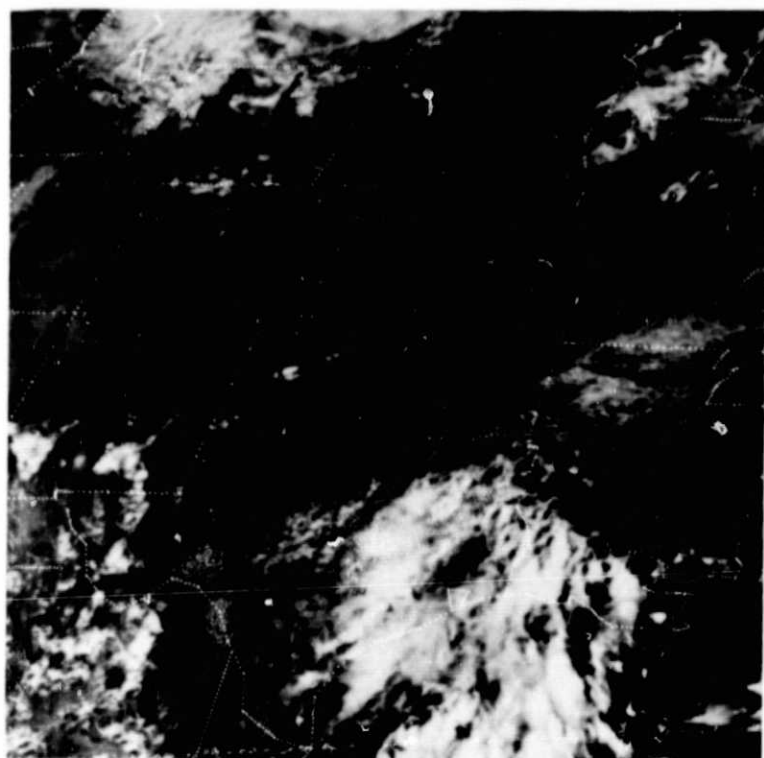


Figure 8 SMS visible image at 2030 GMT (1430 CST) on 24 August 1975.  
Note the line of clouds through the Texas panhandle with  
convective cells in the central panhandle.

ORIGINAL PAGE IS  
OF POOR QUALITY

line in the position indicated in both dew point analyses. The 2035 GMT NWS radar summary in Figure 9 shows the maxima thunderstorm tops in the Texas panhandle at 10400 meters (34000 ft). This convection does exist through 2335 GMT (not shown) with the maximum intensity then mostly near the southern of the two cells in the 2035 GMT radar summary.

The other main indications from satellite-derived parameters of the possibility of severe weather or of any convection in this region are the stability indices. The satellite-derived cross total analysis in Figure 10 shows a local maximum in the Texas panhandle near where the maximum convection does occur. A line of high instability with local perturbations extends up into central Kansas. Similarly, the satellite-derived K value stability index in Figure 11 shows the same features. Here, however, the maxima show up better because of a larger gradient in the whole field. So, these areas of maximum instability do correlate with a general line of convective activity shown in the SMS visible image in Figure 8. Quite strong evidence does therefore exist of the ability of satellite soundings to detect mesoscale conditions at a resolution at least as good as that of surface stations. The rawinsonde stability indices do not show any local maxima as indicated in the satellite data. The rawinsonde K value stability analysis in Figure 12 shows only the general gradient of stability from northwest to southeast associated with increasing low level moisture in this direction.

#### 8.0 CONCLUSIONS

Possibly some of the biggest strides in weather analysis and forecasting in the next few years will be at the mesoscale (25-250 Km). This scale deals with the environmental conditions around severe storms or systems of such storms. Features to be studied usually have some type

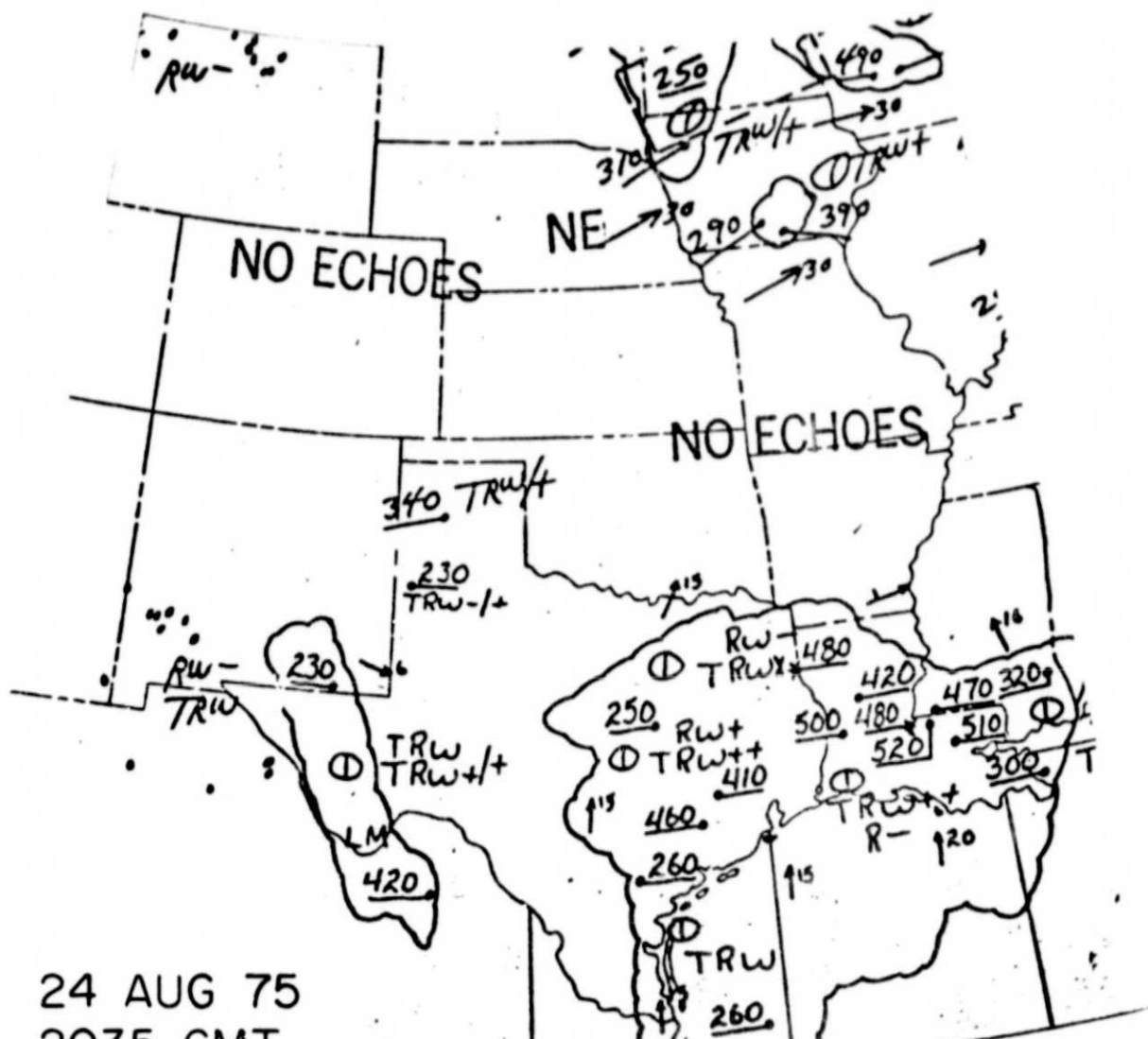


Figure 9. Radar summary at 2035 GMT (1435 CST) on 24 August 1975. Note the moderate size but growing thunderstorms in the Texas panhandle.

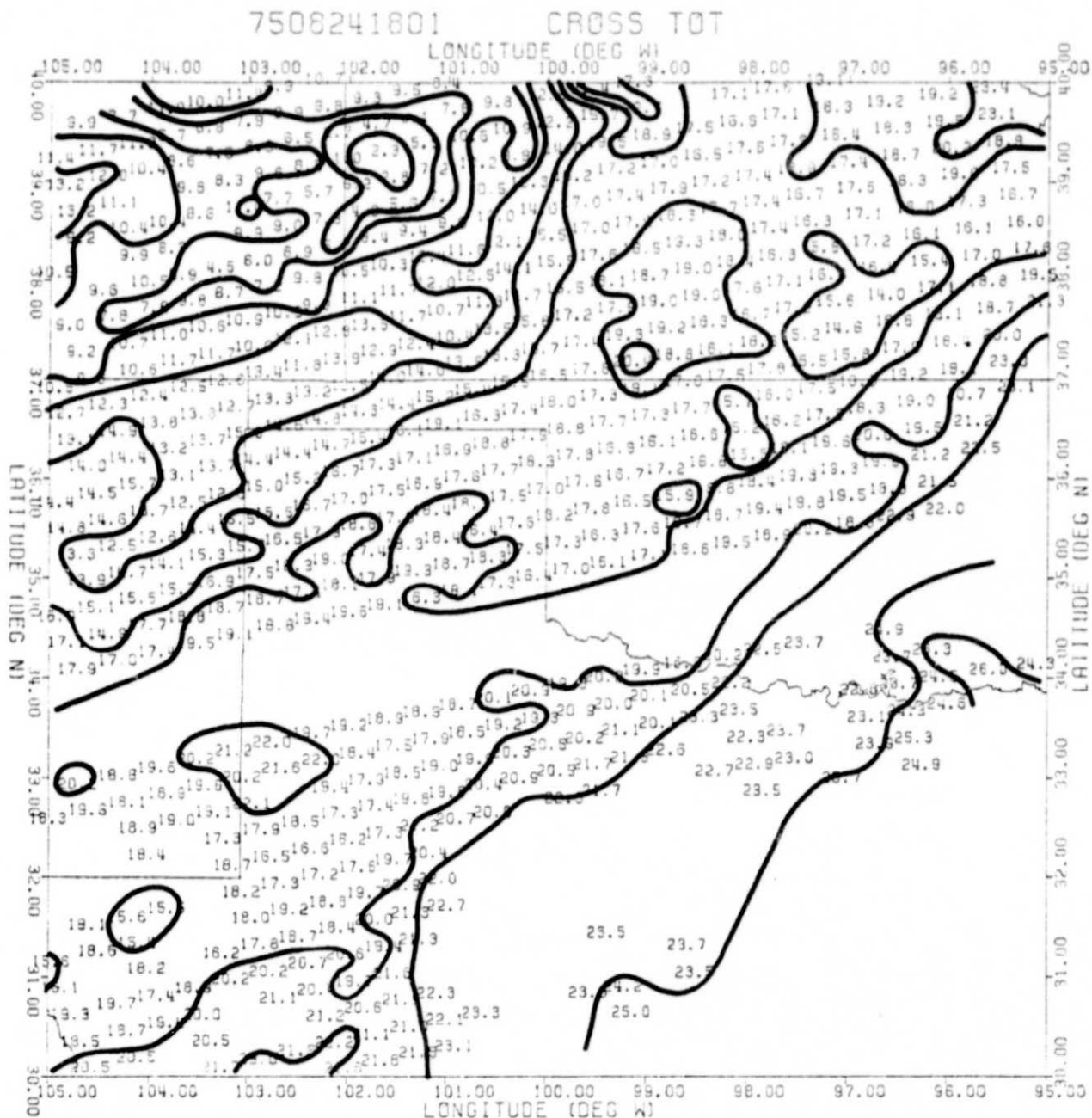


Figure 10. Cross total stability analysis from retrieved HIRS soundings at 1801 GMT on 24 August 1975. Note the line of instability extending through the Texas panhandle and into central Kansas. Contours are every  $2^{\circ}\text{C}$ .

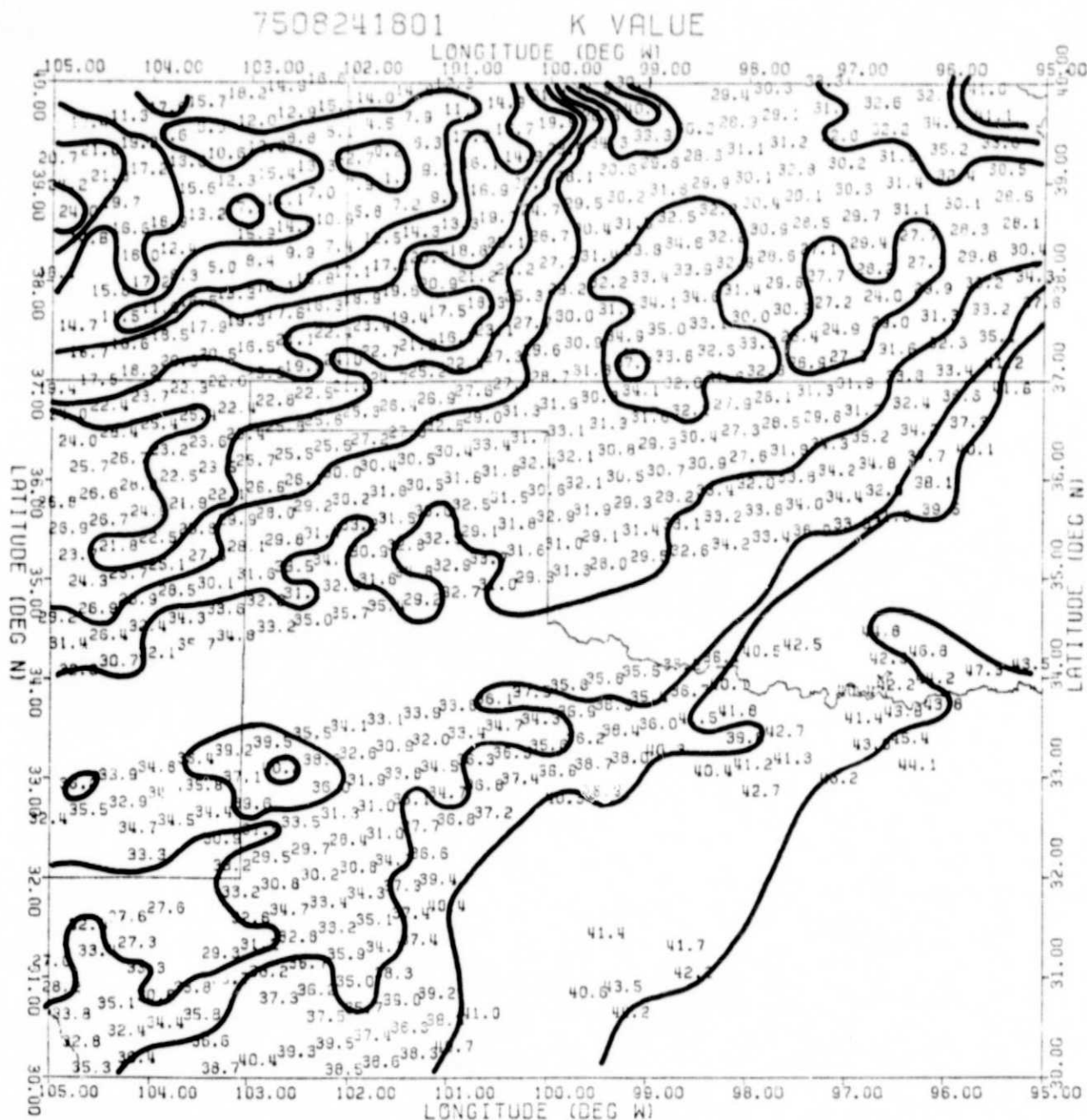
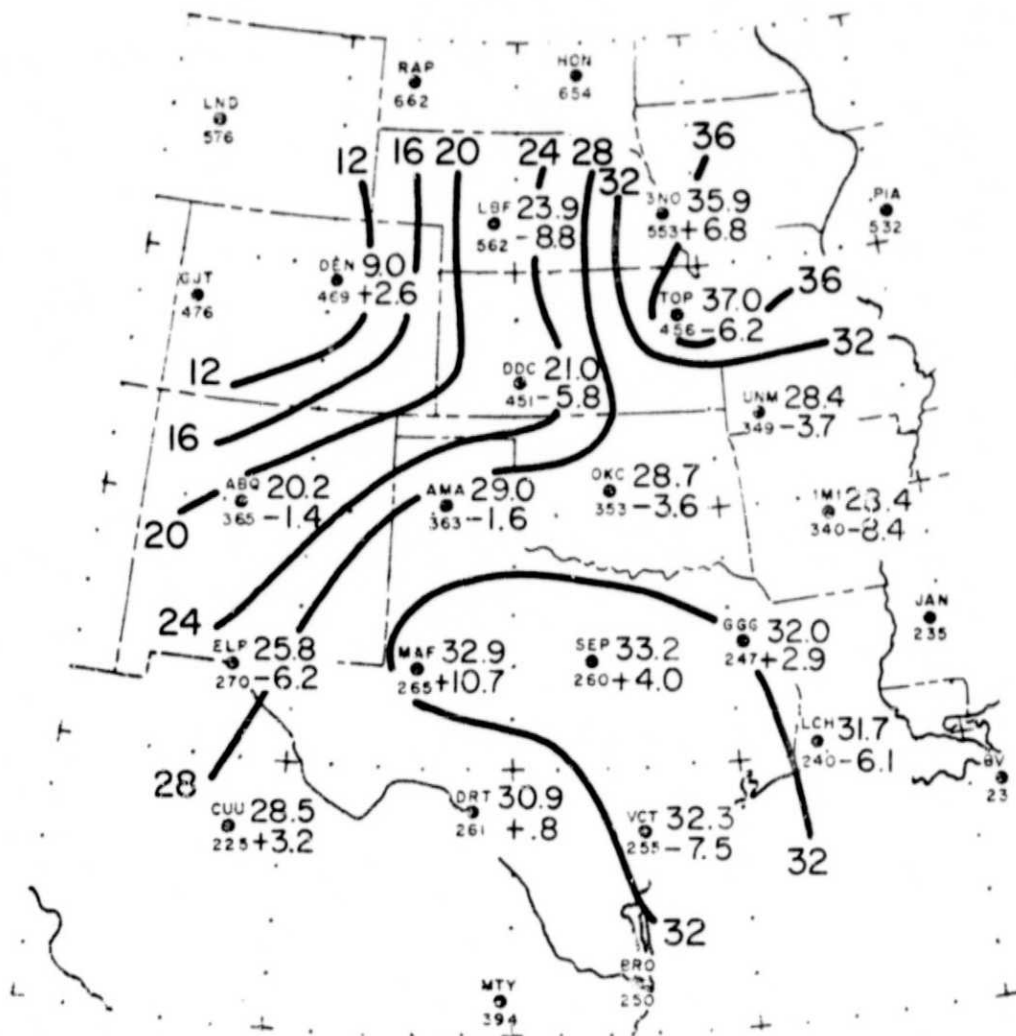


Figure 11. K value stability analysis from retrieved HIRS satellite soundings at 1801 GMT on 24 August 1975. Note the same line of instability as shown in Figure 10. Contours are every  $4^{\circ}\text{C}$ .



24 AUG 75  
1800 GMT INTERPOLATED  
K VALUE (°C)

Figure 12. K value stability analysis from 1800 GMT interpolated values on 24 August 1975 from synoptic rawinsondes at 1200 and 0000 GMT. Upper value is K value, lower value is 12 hour change.

of organization such as along a dry line or mesoscale frontal feature. The actual temperature and moisture structure of those mesoscale features is not very well known. Therefore, the recent emphasis on such programs as SESAME which call for both this type of mesoscale investigation of severe storm situations and a study of tools which will provide what needs to be known.

The HIRS satellite soundings in this study were used at their full resolution of 30 Km (barring clouds). Radiances from the HIRS instrument are capable of producing mesoscale analysis and forecasting parameters necessary for severe storm research. The use of such new tools is a goal of SESAME.

The dual retrieval scheme used here was designed specifically to extract the lower tropospheric parameters necessary for severe storm forecasting. Parameters such as total precipitable water, surface dew point temperatures, and stability indices were successfully retrieved. These satellite-derived parameters were well correlated with their interpolated counterparts from NWS rawinsondes. This, of course, is not a reliable indication of the true quality of the mesoscale analyses which were derived from the satellite radiances. The intrinsic noise levels of the derived parameters by structure function analysis were also very low. This gives an indication of the quality of the mesoscale analyses. The true value of satellite data will only be shown in mesoscale situations where their high horizontal resolution is an advantage. In this role the analyses seem to show small-scale features on the order of 100 km. These perturbations on the mesoscale dry line for this one case study day, 24 August 1975, do appear to be associated with the location of later convective developments. The dry line is located by the satellite

moisture analysis with the same precision as surface observations, but smaller local maxima of precipitable water and pockets of instability are seen only in the satellite data. These local maxima do correlate with the most intense areas of convective development  $2\frac{1}{2}$  hours later, even though this is a rather suppressed day for activity in this region.

The results do seem to be valuable, but further testing will be needed. By applying this type of analysis to more situations a confidence should be built up in the usefulness of satellite-derived parameters at the mesoscale. Further testing and improvements could include a cloud model to avoid the present limitation of only clear soundings being available. Other than that main improvement, there is the possibility of using more of the information which is available from the unused HIRS radiances, such as the partly redundant shortwave  $\text{CO}_2$  channels which were not used in this retrieval scheme. Likewise similar improvements may be possible by using other pieces of information from new satellite instruments. To be able to use the extra channels available on TIROS-N, which was launched in fall 1978, will require only slight modification of the retrieval scheme. An increase in the number of independent or partially independent pieces of information can hopefully improve results.

## REFERENCES

Gary, J. P., 1977: AOIPS data base management systems support for GARP data sets, NASA Technical Memorandum 78042, 36 pp.

Gandin, L. S., 1963: Objective analysis of meteorological fields. Translated from Russian, Israel Program for Scientific Translations, Jerusalem, 242 pp. (NTIS Ref: TT-65-50007).

Hillger, D. W. and T. H. Vonder Haar, 1979: An analysis of satellite infrared soundings at the mesoscale using statistical structure and correlation functions. J. Atmos. Sci., 36, 287-305.

Hillger, D. W. and T. H. Vonder Haar, 1977: Deriving mesoscale temperature and moisture fields from satellite radiance measurements over the United States. J. Appl. Meteor., 16, 715-726.

Kelly, G. A. M., G. A. Mills and W. L. Smith, 1978: Impact of Nimbus-6 temperature soundings on Australian region forecasts. Bull. Amer. Met. Soc., 59, 393-405.

Lilly, D. K. (Editor), 1977: Project SESAME (Severe Environmental Storms and Mesoscale Experiment), Planning Documentation Volume NOAA/ERL, Boulder, CO, 308 pp.

Lilly, D. K. (Editor), 1975: Open SESAME, Severe environmental storms and mesoscale experiment, Proceedings of open meeting, Boulder, CO, 4-6 Sept. 1974, June, 499 pp. (Government Pub. Order No. C55.602:Sr8).

Miller R. C., 1972: Notes on analysis and severe-storm forecasting procedures of the Air Force Global Weather Central, AWS Technical Report 200.

Project SESAME, 1976: (Severe Environmental Storms and Mesoscale Experiment), Project Development Plan, NOAA/ERL, Boulder, CO, 60 pp.

Rhea, J. O., 1966: A study of thunderstorm formation along dry lines, J. Appl. Meteor., 5, 58-63.

Schaefer, J. T., 1974: The life cycle of the dry line, J. Appl. Meteor., 13, 444-449.

Schaefer, J. T., 1973: The motion of the dry line, Preprints, Eighth Conference on Severe Local Storms, American Meteorological Society, Denver, CO, 104-107.

Schwalb, A., 1978: The TIROS-N/NOAA A-G satellite series, NOAA Technical Memorandum, NESS 95, 75pp.

Smith, W. L., 1970: Iterative solution of the radiative transfer equation for the temperature and absorbing gas profile of an atmosphere. Appl. Opt., 9, 1993-1999.

Smith, W. L., C. M. Hayden, H. M. Woolf, H. B. Howell, and F. W. Nagle, 1978: Remote Sounding of the Atmosphere, COSPAR, June, Innsbruck.

Smith, W. L., H. M. Woolf, P. G. Abel, C. M. Hayden, M. Chalfant, and N. Grody, 1974: Nimbus-5 sounder data processing system, Part 1. NOAA Technical Memorandum NESS 57, 99 pp. (NTIS Ref: COM-74-11436/4GI).

Smith, W. L., P. G. Abel, H. M. Woolf, A. W. McCulloch, and B. J. Johnson, 1975: The high resolution infrared radiation sounder (HIRS) experiment, The Nimbus-6 User's Guide, 37-58. (NTIS Ref: N76-31256/OGI).

Tracton, M. S., and R. D. McPherson, 1977: On the impact of radiometric sounding data upon operational numerical weather prediction at NMC. Bull. Amer. Meteor. Soc., 58, 1201-1209.

Wark, D. Q., J. H. Lienesch and M. P. Weinreb, 1974: Satellite observations of atmospheric water vapor, Applied Optics, 13, 507-511.